Received: 1 March 2022 | Revised: 31 May 2022 | Accepted: 3 July 2022

DOI: 10.1002/aff2.66

AQUACULTURE, FISH and FISHERIES Open Access

WILEY

CASE STUDY

Automated image analysis as a tool to measure individualised growth and population structure in Chinook salmon (*Oncorhynchus tshawytscha*)

Nicholas P. L. Tuckey[1] | **David T. Ashton**[1] | **Jiakai Li**[2] | **Harris T. Lin**[2] | **Seumas P. Walker**[3] | **Jane E. Symonds**[3] | **Maren Wellenreuther**[1,4]

[1]The New Zealand Institute for Plant and Food Research Ltd, Nelson, New Zealand

[2]The New Zealand Institute for Plant and Food Research Ltd, Auckland, New Zealand

[3]Cawthron Institute, Nelson, New Zealand

[4]School of Biological Sciences, The University of Auckland, Auckland, New Zealand

Correspondence
Nicholas P. L. Tuckey, The New Zealand Institute for Plant and Food Research Ltd, Nelson, New Zealand.
Email: Nicholas.Tuckey@plantandfood.co.nz

Funding information
Ministry of Business, Innovation and Employment, Grant/Award Number: CAWX1606; Ngā Pou Rangahau platform

Abstract

Selective breeding programmes depend on high-quality measurements of phenotype and genotype with repeated individualised phenotype measurements throughout the life cycle being optimal. Recent advances in electronics and computer vision technologies offer opportunities to improve both the quality, quantity and individualisation of repeated phenotypic measurements, but remain underutilised in aquaculture breeding programmes. In this study, we compare manual measurements of phenotypic traits of Chinook salmon (*Oncorhynchus tshawytscha*) with digital images and an automated software analysis pipeline written in the Python® programming language using the OpenCV machine vision library. Manual measurements of length, girth and weight of passive integrated transponder-tagged individuals were compared with image-based measures of 738 individuals over a time span from June–December 2019. Linear regressions showed strong correlations between manual and automated measurements for fork length, girth and weight (R^2 = 0.989, R^2 = 0.918, R^2 = 0.987, respectively). Image-based software measurements proved powerful for tracking general population changes in growth over the study period while retaining insights about subpopulations deviating from the average (e.g. losing weight). Taken together, our study demonstrates that image-analysis can be used to estimate fish growth traits with a high degree of precision, requires reduced labour and demonstrates that additional knowledge can be gained through tracking individuals throughout production to harvest.

KEYWORDS
breeding programme, computer vision, growth, morphometric software, population dynamics, salmon

1 | INTRODUCTION

Selective breeding programmes for aquaculture are a relatively recent endeavour compared with the long history of terrestrial plant and animal breeding programmes, which have facilitated increased agricultural productivity and viability (Gjedrem & Robinson, 2014; Teletchea & Fontaine, 2014). The aim of breeding programmes is to select and breed superior animals so that resulting offspring will perform more efficiently under future production circumstances. One of the main phenotypic performance metrics in aquaculture breeding and production is growth, as improving growth rate is expected to increase farm profit through a reduction in grow-out time, thus increasing annual production and economic returns (Gjedrem & Rye, 2018; Houston & Macqueen, 2019; Murata et al., 1996).

Capturing phenotypic measurements from populations of finfish in research environments, despite many recent advances (Shortis et al., 2016; Zion, 2012), is typically carried out manually using tools such as balances, tape measures and/or fish boards (some of which are now capable of digitally logging information). Although some examples of digital image-based phenotyping technologies focused on scientific use have recently been developed (Andrialovanirina et al., 2020; Fernandes et al., 2020; Navarro et al., 2016; SriHari et al., 2019), these do not allow for rapid data capture from live animals. Many commercial systems are industrially focused (e.g. Vaki Aquaculture Systems Ltd., Iceland) and, although capable of counting and/or collecting fish size measurements using machine vision technologies, these systems are cost prohibitive for most researchers and small-scale producers. Also, they do not allow for the same individual fish to be assessed throughout growth and life cycles. Furthermore, recent studies have shown that the measurement approach used to infer biomass and population structure (i.e. a subsampling of the population or the measurement of every individual) needs to be carefully designed if the information collected is to accurately represent the population (Aunsmo et al., 2013; Nilsson & Folkedal, 2019). Finally, a full understanding of the population dynamics in a culture environment is only possible if each individual can be identified and repeatedly measured throughout their growth cycle, such as through the use of passive integrated transponder (PIT) tags or other identification systems such as biometrics (Schraml et al., 2021; Stien et al., 2017). The value of precision fish farming (in which individuals are tracked) is currently topical with regard to production systems, and this level of information is hugely valuable. For example, in commercial aquaculture breeding programmes, growth is usually measured at least 1–2 times during the lifetime of an individual and typically involves the manual measurement of weight and total length (Kause et al., 2006; Navarro et al., 2009). Ensuring accurate phenotypic measurements while streamlining the data capture process is a priority when thousands of breeding candidates need to be assessed.

Conventional manual techniques for assessing fish growth are usually time-consuming, costly and stressful for the animal (Iversen et al., 2003). Even with the effective use of anaesthesia and good husbandry practices, measurement is a stressful event and for both cost and ethical reasons needs to be either non-intrusive (i.e. no removal from the water) or as infrequent as possible. Image-based methods may help to reduce the handling time of fish, as one image can simultaneously capture and store a phenotypic record while allowing subsequent measurement of many phenotypic traits. The value of image-based methods for morphometric studies of fish has been highlighted in previous studies based on its performance and the accuracy of the morphometric measurements (Takacs et al., 2016).

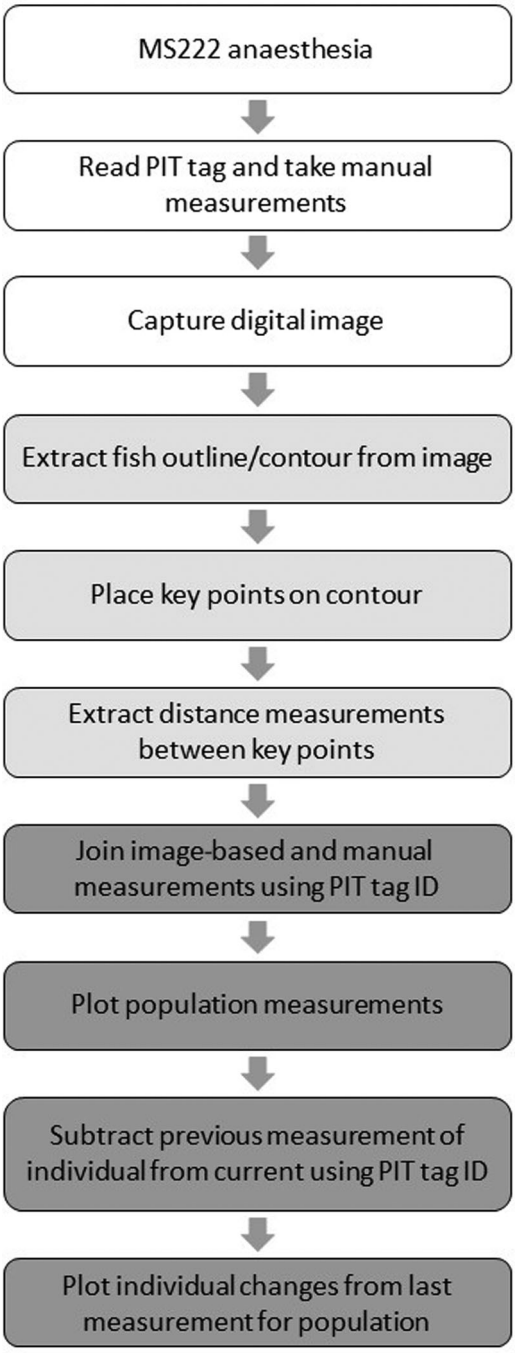

FIGURE 1 Flow diagram of the measurement workflow used in this study. White boxes indicate the physical workflow, light grey boxes show the image processing procedures, and dark grey boxes show the data processing and visualisation procedures

TABLE 1 Date, tank allocation, number of individuals and mean weights of Chinook salmon measured between June and December 2019 using digital images and manual measurements for this study

Sampling date	Tank	Number of samples	Mean weight ± SD (g)		
26/06/2019	1	124	1027	±	208
26/06/2019	2	125	1037	±	212
12/08/2019	1	88	1553	±	312
12/08/2019	2	88	1599	±	326
3/10/2019	1	87	1921	±	449
3/10/2019	2	88	2028	±	442
20/11/2019	1	68	2212	±	586
3/12/2019	2	70	2216	±	539

Here, we test the feasibility and accuracy of using a simple light box and camera system to capture digital images and an automated image-analysis software pipeline (Morphometric software) to measure individualised growth traits and population structure in Chinook salmon (*Oncorhynchus tshawytscha*), New Zealand's only commercial finfish aquaculture species (Aquaculture New Zealand, 2020). We assessed manual measurement methods paired with image-based methods to compare and contrast the accuracy and performance of the two approaches for measuring captive salmon populations.

2 | MATERIALS AND METHODS

2.1 | Chinook salmon culture

Chinook salmon (*O. tshawytscha*) were maintained at the Cawthron Institute's Finfish Research Centre in Nelson, New Zealand. The fish were reared in a saltwater recirculating aquaculture system at 17 ± 0.5°C with a minimum dissolved oxygen level of 9 mg/L. At the point of first data collection in June 2019, the fish were split between two 8 m^3 tanks containing 124 and 125 individuals with mean fish sizes of 1027 ± 208 g (±SD) and 1037 ± 212 g, respectively. A total of four assessments were carried out and all fish were measured at each assessment. Fish numbers were reduced randomly throughout the measurement period to maintain an acceptable biomass in the tanks, and as such at the fourth and final data collection point in November/December 2019 there were 68 and 70 fish remaining in the two tanks, with mean weights of 2212 ± 586 g and 2216 ± 539 g, respectively (Table 1). Each fish was individually tracked using a PIT tag.

2.2 | Manual fish measurements

A flow diagram of the measurement workflow used in this study is shown in Figure 1. Fish were crowded and dip netted from their tanks into a bath of anaesthetic (100 L of 65 mg/L tricaine methanesulfonate, Syndel, WA, USA) and maintained there until they had reached stage 3 anaesthesia (Stoskopf & Posner, 2008). The fish were then removed from the anaesthetic bath, scanned with an Avid PowerTracker 6 PIT tag scanner (Avid Identification Systems, Inc. CA, USA) and placed on a fish board on top of a digital balance (Ohaus Corporation, NJ, USA). Weight and length were then obtained followed by the girth, which was measured around the largest circumference (just anterior to the dorsal fin) using a flexible tape measure. Immediately after the fish were manually measured, a digital image of each individual was captured. The time from the fish being netted from the tank to the completion of the digital image capture was recorded and was generally between 30 and 60s. However, the times for each measurement step within this process were not recorded. No mortalities were observed as a result of these handling procedures.

2.3 | Digital image capture

Digital images were captured using a custom-built light box (Figure 2). The box was constructed out of folded and welded 3 mm thick white polypropylene sheet from which an enclosed rectangular box 600 mm × 600 mm × 1000 mm (W × D × H) was formed. A further sheet of 1.6 mm white polypropylene cut to 1400 mm × 600 mm (L × W) was bent and fitted within the rectangular box to form an oval arch on which the light strips were mounted. A central 80 mm round hole was cut in the centre of the arch for the camera lens to pass through. Four M10 nylon bolts and wingnuts (two per side) penetrated the lower ends of the arch where it contacted the box to secure it. The bolts passed through four vertical channels (two per side; Figure 2b) cut in the sides of the light box which ran from 100 to 600 mm above the base. This allowed height adjustment for the lighting and camera. Four 600 mm long ribs were attached to the lower surface of the arch using countersunk stainless-steel screws. These were run from the front to the back of the unit at 70 and 625 mm, measured from the bases of the arch on both sides, forming a symmetrical structure. Four 500 mm lengths of Standard Illuminant CRI 98 D50 5000K LED 24 V flexible strip lighting (Beijing Yuji International Co., Ltd, Beijing, China) were installed between the ribs on each side of the structure. The first strip was placed 70 mm above the lower rib and at 63 mm intervals thereafter. A sheet of polymer light diffuser (Rosco Cinegel 3026; Rosco Laboratories Inc., CT, USA) was also installed between the ribs on each side of the unit ensuring that all LEDs were covered, to reduce specular

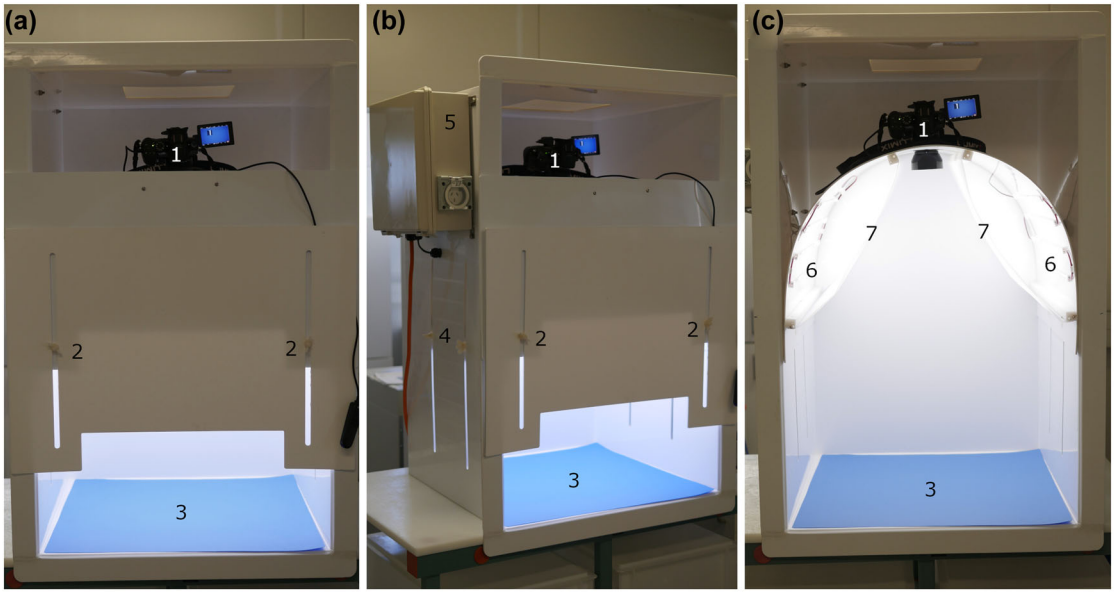

FIGURE 2 Digital image capture system used for data acquisition in this study showing (a) the front profile of the unit, (b) the side profile, and (c) the front profile with the face plates removed. The major components of the system are labelled (1) camera, (2) wingnuts for the sliding adjustable face plate, (3) matte blue polypropylene background, (4) wingnuts and channels for adjusting the light arch height, (5) electrical box containing LED drivers, (6) LED light strips, (7) flexible polymer diffusers

reflections. The four LED strips on each side of the unit were wired in series using Two Pin Piercing Grip Strip Connectors and 20 AWG wire and connected back to an LED driver (Beijing Yuji International Co.) contained in a weatherproof electrical box. The electrical box was supplied with mains electricity (240 VAC) through a 5 m weatherproof electrical lead and plug. The total cost of parts including the plastic engineering, LEDs, drivers and electrical work (excluding the camera) was approximately NZ$2500.

A 16-megapixel Panasonic Lumix DMC-GH4 camera (Panasonic Corporation, Osaka, Japan) fitted with a Panasonic Leica DG Summilux 25 mm ASPH lens was mounted on a Manfrotto 496RC2 compact ball head. The camera was arranged so that the lens passed vertically through the 80 mm round hole in the centre of the light arch, and the top of the camera faced the front of the unit. A remote shutter button (covered with a polyethylene zip-lock bag to provide some water protection) was connected to the camera to allow convenient image capture. A 0.6 mm thick matte blue polypropylene sheet was cut to fit the base/stage of the light box to provide a contrasting background colour for the subjects in the digital images. The camera was operated in manual mode and white balanced using a 200 mm × 200 mm white Teflon square. The lens aperture was set to f16 and the ISO speed to 800. The lighting levels and shutter speed were adjusted to provide RGB values of approximately 185 on the red, green and blue channels of the digital images, respectively, as measured against the white squares of a ColorChecker SG colour calibration target (X-Rite, Inc., MI, USA). As such, the unit described here is capable of quantitative colour measurements. These were not a focus of this study however. Here, a shutter speed of 1/80 s was used. To capture images, fish were placed inside the light box with their left side facing up towards the camera and their head to the left of the frame.

2.4 | Digital image analysis

The digital images were analysed using Plant & Food Research's Morphometric Software, which is a collection of software modules for image analysis focused on marine organisms written in the Python programming language using the OpenCV computer vision library (Bradski, 2000). Briefly, the contour (outline) of each fish was extracted, and 11 reference points were algorithmically placed on the outline (Figure 3). These software operations were initially established using image thresholding and contour feature detection algorithms (used for this analysis), but more recently conducted using MXNet-based machine learning models (The Apache Software Foundation, DE, USA) similar to those described by Fernandes et al. (2020). From these reference points, a series of measurements was obtained, including body side area, fork length and body height at 0.25, 0.5 (mid-point) and 0.75 positions relative to fork length. Measurements were initially captured as pixels but were converted to millimetres using a 150 mm scale bar present in each image.

2.5 | Data management, statistical analysis and visualisation

Analyses were carried out using Python 3.8.5 (Anaconda Software Distribution, 2016) with the pandas 1.1.1 library (The Pandas Development Team, 2020) for data management, the statsmodels 0.12.0 library (Seabold & Perktold, 2010) for linear regression, and the seaborn 0.11 and matplotlib 3.3.2 libraries (Hunter, 2007; Waskom and the Seaborn Development Team, 2020) for data visualisation. With fish masses constrained in this study, an ordinary least squares (OLS) regression

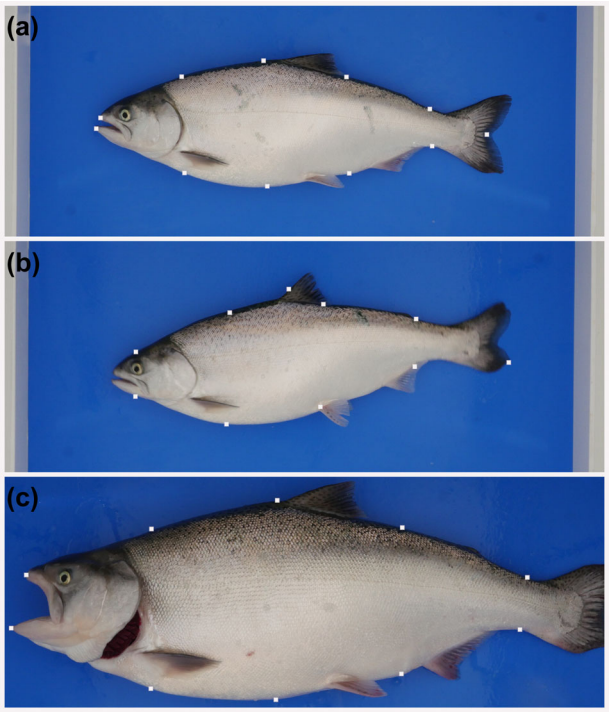

FIGURE 3 A visualisation of the placement of the 11 reference points generated by the Morphometric software to automate Chinook salmon size measurements. (a) An example of correct placement of the reference points by the software. (b) An example of incorrect placement of the reference points by the software with motion blur a probable cause (two occurrences; $n = 738$). (c) An example of missing reference points due to incorrect subject placement during image capture (one occurrence)

was used for simplicity. As sample measures were repeated and paired, and the population distributions were not normal, pair-wise testing of manual measures and image-based measures was conducted in R (R Core Team, 2021) using Wilcox rank sum tests with *p* value adjustments as in Benjamini and Hochberg (1995). To allow this testing, predicted weight and girth were calculated from the fish body side area and body height at the mid-point of fork length measurements extracted from the digital images using the OLS regression equations.

3 | RESULTS

Between June 2019 and December 2019, a total of 738 measurements of Chinook salmon sizes were captured both through manual measurements and with associated digital images (Table 1) using a custom-built light box (Figure 2). An example image, including the reference points (white squares) used to extract automated measurements is shown in Figure 3. Of these measurements, 138 were captured in November/December 2019 of individuals that had been present in the population throughout the study (i.e. repeatedly sampled).

In June 2019, the fish present in the monitored population had a range of masses between 437 g and 1742 g with a mean of 1032 ± 210 g (± SD). By November/December 2019, the mean fish mass had increased to 2214 ± 516 g with a range of masses between 924 g and 3794 g. As such, the total range of fish masses used to establish a mass prediction model based on information extracted from digital images of Chinook salmon was 437–3794 g (Figure 4). An ordinary least squares linear model was fitted to these data, which returned an R^2 value of 0.987.

Linear models were also established to relate digital image-based fork length measurements with manual fork length measurements ($R^2 = 0.989$), and the digital body height measurement at the mid-point of fork length to the manual girth measurements. The latter resulted in a lower R^2 value of 0.918, predominantly owing to some notable outliers.

Secondary visualisations of the population data were carried out to establish if the measurements taken from digital images could generate detailed population structures comparable to those captured through the manual measurements. In this case, violin plots for weight, fork length and girth from the two measurement types were generated and placed together (Figure 5). A high degree of similarity in the distributions for the image-based and manual measurements was notable. Pair-wise Wilcoxon rank sum tests were conducted to establish if the measures from the manual and image-based measures were equivalent. In the case of the image-based length measures, the median values were 358 mm compared to 356 mm ($p < 0.05$) for June, 415 mm compared to 407 mm ($p < 0.001$) for August, 454 mm compared to 445 mm for October, and for the final measurement, 483 mm compared to 470 mm ($p < 0.001$). For girth the image-based predictions significantly differed only for the October measurements with the median being 347 mm compared to 356 mm ($p < 0.05$) for the manual measurements.

Finally, the changes relative to the previous measurement for each individual fish in the population were calculated by subtracting each individual's measurement from that captured during the previous sampling, and these data were replotted using violin plots (Figure 6). For the manual weight measurements and image-based weight predictions, the distributions showed a high degree of similarity and there were no significant differences between the two measurement types. The image-based length measurements showed notable outliers in August and November/December but were otherwise similar. Median length changes were 54 mm compared to 49 mm in the June to August interval ($p < 0.001$) and 29 mm compared to 25 mm for the October to November/December interval. The girth measurements showed the highest disparities, with outliers influencing the distributions in both the manual measurements and the digital image-based girth predictions. Changes in median girth for the image-based and manual girth measurements were 40 mm compared to 38 mm for the June to August interval, 22 mm compared to 33 mm for the August to October interval and 12 mm compared to 7 mm for the October to November/December interval for the image based and manual measurements, respectively. These medians were significantly different ($p < 0.001$) in all cases. This shows that some error was accumulated through the prediction calculations. Despite this, there was still a high degree of similarity in the locations of the population bulges in the plots generated from the two measurement types.

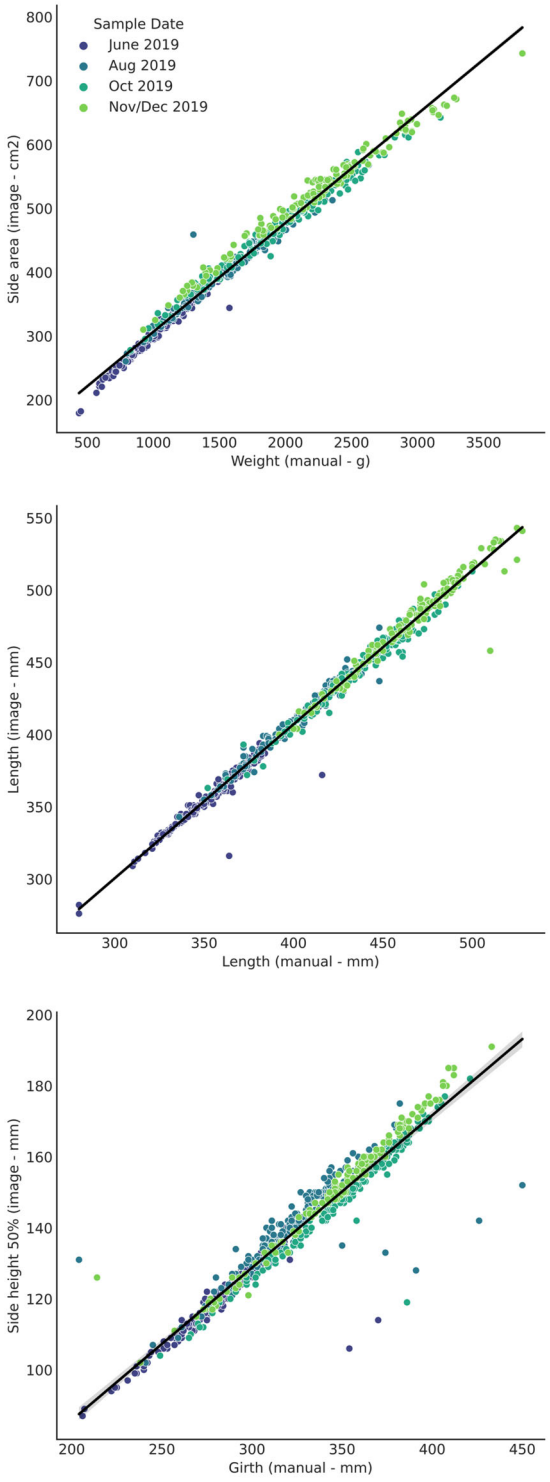

FIGURE 4 Chinook salmon size measurements ($n = 738$) captured between June and December 2019 using digital images (left axes) and manual measurements (bottom axes). Top panel: image-based side area (cm) and weight (g) (Linear Regression: $y = 0.171x + 136.078$; $p < 0.001$; $R^2 = 0.987$). Middle panel: image-based fork length (y) and manual fork length (x) (linear regression: $y = 1.066x - 19.283$; $p < 0.001$; $R^2 = 0.989$). Bottom panel: image-based side height at 50% of fork length (y) and girth (x) (linear regression: $y = 0.429x - 0.052$; $p < 0.001$; $R^2 = 0.918$)

By the end of the experiment (December 2019), a bimodal distribution in the population was seen in both the change in weight and the change in girth measures detected using both data capture methods (Figure 6). As all individuals were PIT tagged and measured multiple times, we were able to determine that this bimodal population distribution was due to weight loss in a proportion of the population.

4 | DISCUSSION

Our study compared manual growth measurements with digital image analysis. The results demonstrated the utility of computer vision technology to improve phenotypic data capture of teleost fish for scientific studies and breeding programmes where sample throughput requirements are relatively low, but the need for accurate data is essential. This image-based growth assessment for Chinook salmon showed that automated image-based measurements were comparable to those collected manually. Images also provide a good method of archiving phenotypic information of individual fish, which, when coupled with individual identification of individuals, either through manual or image-based tags, are an information-rich resource to inform the breeding and production of fish in aquaculture.

4.1 | Fish husbandry and workflow

The imaging units built for this study were designed as a cost-effective means of enabling studies that require high-quality repeated measurements of fish phenotype. The design is similar to those described previously (Balaban, Chombeau, et al., 2010; Balaban, Ünal Şengör, et al., 2010; Luzuriaga et al., 1997), but, although the units require mains (240 V) electricity, they are portable and can be used beside fish tanks and in wet work areas. Low-cost polypropylene was used as the main construction material, and for the coloured removable background—which can be easily sterilised to manage biosecurity risks. Furthermore, the automation at point of image-capture eliminated the need for paper-based records in fish measurement operations, which reduced staff requirements. The workflow had two primary limitations. (1) The use of a stand-alone digital camera generates some work flow inconvenience when collating data from multiple sources, and (2) the manual handling of fish limited the sample capture throughput. The overall throughput of our measurement workflows in this study was constrained (approximately 65 fish per hour) due to the need to collect manual fish measurements in addition to image-based measurements for comparison. However, with suitably designed husbandry and anaesthesia in place, we estimate a throughput of 3–6 fish per minute (approximately 250 fish per hour) per imaging unit could be achieved.

4.2 | Measuring fish traits from digital images

For the software-based analysis of digital images, our selection of Python (i.e. an accessible programming language) for automation tasks

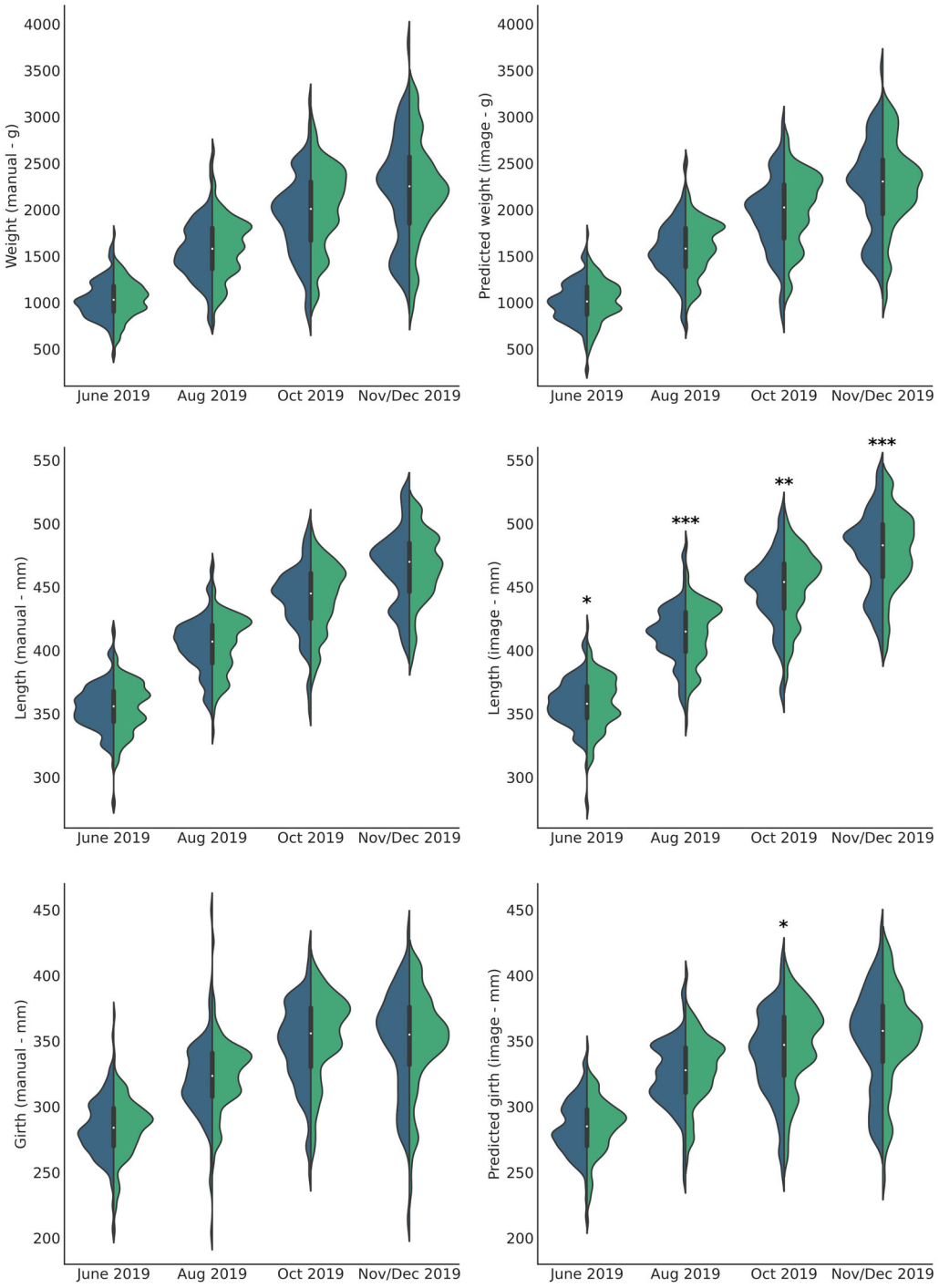

FIGURE 5 Chinook salmon size measurements and population structures captured between June and December 2019 using manual measurements (left panels) and digital image-based measurements (right panels). The violin shapes are split to define the two separate culture tanks; tank 1 = blue and tank 2 = green. Results from pairwise Wilcoxon rank sum tests comparing matched manual and image-based measures are displayed (*$p < 0.05$; **$p < 0.01$; ***$p < 0.001$). Median image-based length measurements were found to range between 2 and 13 mm (for June 2019 and December 2019, respectively) greater than their matched manual measurements

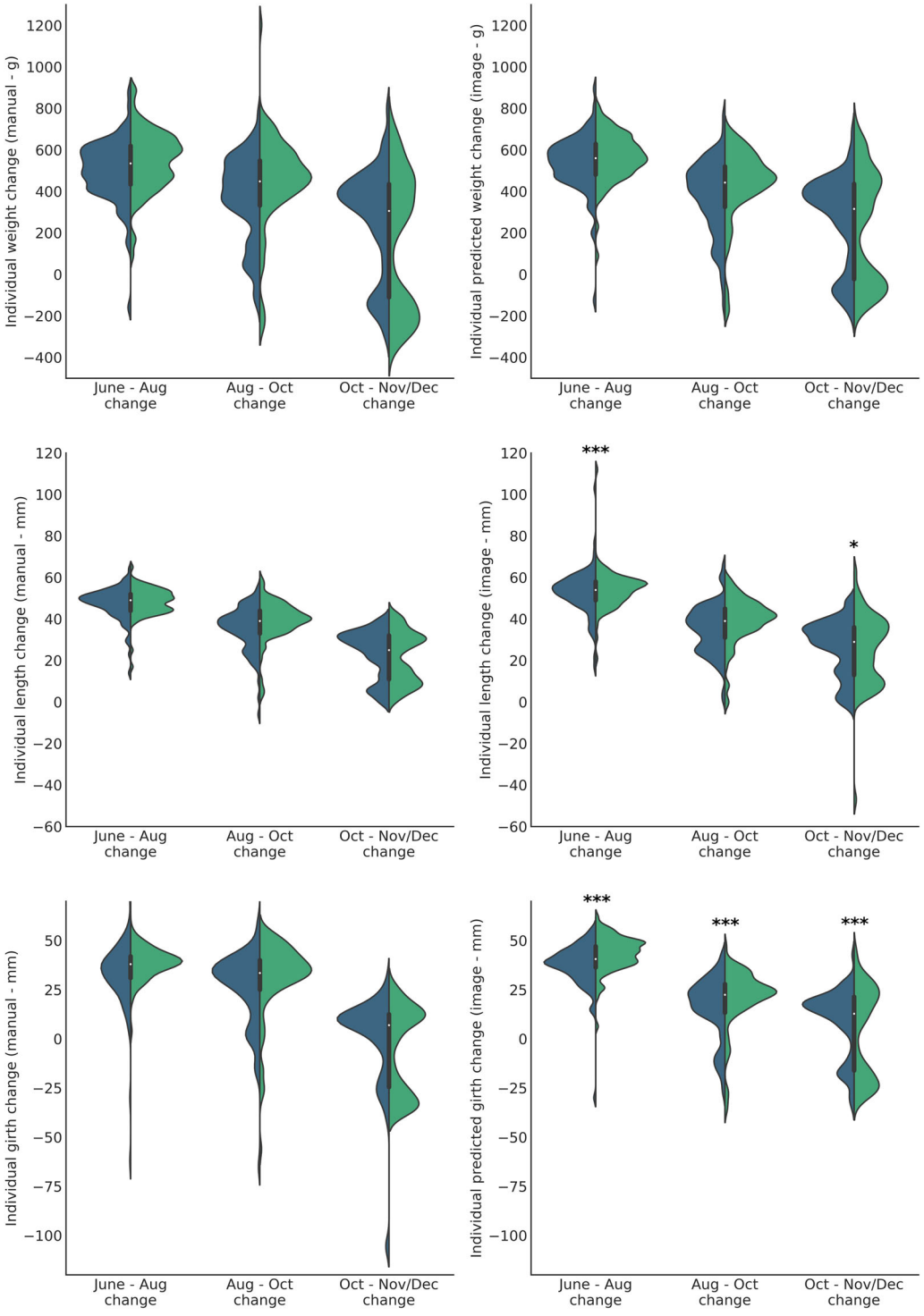

FIGURE 6 Chinook salmon size measurements and population structure captured between June and December 2019 using manual measurements (left panels) and digital image-based measurements (right panels) displayed as the change in size of each individual fish from the previous measurement. Individual fish tracking was conducted using passive integrated transponder (PIT) tags. The violin shapes are split to define the two culture tanks used; tank 1 = blue and tank 2 = green. Results from pairwise Wilcoxon rank sum tests comparing matched manual and image-based measures are displayed (*$p < 0.05$; **$p < 0.01$; ***$p < 0.001$)

was made with the aim of initiating the construction of simple maintainable automated software pipelines (Morphometric software) for finfish phenotype measurements. Once digital images of each sampled fish had been captured using a controlled environment and digitally archived with their metadata, the 150 mm scale bar present in each image allowed a pixel to millimetre relationship to be easily established. This relationship is derived from a combination of the focal length of the camera lens and distance of the lens from the subject in the image. In a stable imaging system, the pixel to millimetre relationship is very consistent. The unit used here was designed with a height adjustable arch containing the lighting and camera. As such, this relationship was established and checked for each sampling session and was consistent at 8.3 pixels/mm for the 4608 × 2592 pixel images captured across all the sampling sessions. The scale bar included in each image is a common technique for establishing and verifying dimensions in digital images (Balaban, Chombeau, et al., 2010) and allows this relationship to be checked and verified in any image either manually (by a person using basic image viewing and editing software) or using an algorithm. The effectiveness of using digital images to establish size and colour measurements for fish has been demonstrated by a number of previous studies though with varying levels of accuracies (Balaban, Chombeau, et al., 2010; Balaban, Ünal Şengör, et al., 2010; Bravata et al., 2020; Sengor et al., 2019; Viazzi et al., 2015). Prediction of fish length (mean error 7.6%), weight and girth have previously been demonstrated in multiple species models (Bravata et al., 2020). With respect to image segmentation, reference point placement and morphometric measurement, studies by Navarro et al. (2016) and Fernandes et al. (2020) have effectively validated similar approaches. The results presented here are comparable to these studies on other species but demonstrate that for a single species, simple statistical relationships between manual and image-based measurements can be effectively established.

4.3 | Comparing the performance of digital image-based and manual measurements

Predicted weight and length measurements from digital images showed a very high correlation with manual measurements (R^2 values of 0.992 and 0.989, respectively). These relationships have been well established in previous studies (Balaban, Ünal Şengör, et al., 2010; Beddow et al., 1996; Fernandes et al., 2020; Shortis et al., 2016). Measurements of salmon girth were modelled against the mid-point of body height, which had a lower R^2 value of 0.918. This measurement is less commonly captured, however, and in most use cases the predicted girth values would be of adequate precision. As such, we have demonstrated that the precision of the data generated through automated digital image analysis of Chinook salmon is comparable to that of manual workflows and therefore could replace tools frequently used for such tasks, such as manual balances and fish measurement boards.

The capture of digital images in this study allowed the outliers visible in the weight and length regressions to be traced back through the workflow to determine if they were a product of errors in the measurement workflow or of biological origin. With archived images, the measurements can be re-conducted (manually if needed). In the regressions conducted for weight, there were two outlying points, and for length there were three outlying points (Figure 4). These were manually traced and linked to four measurements—all of which were best explained by measurement error. One of these was likely due to an inaccurate manual weight measurement (1303 g measured manually and 1935 g estimated based on the measured fish side area), one was due to an image capture error (a fish tail falling outside the frame; Figure 3c), and two were due to inaccurate algorithmic placement of the key points used to calculate measurements (e.g. Figure 3b). In the case of the outliers, the errors in digital length measurement were between 44 and 52 mm smaller than the matching manual length measurements. There were 11 outlying measurements for the mid-point body height and girth regression (Figure 4). These were not manually traced, but a pattern of six points offset and running parallel to the regression is suggestive of a systemic measurement error. As such, the predicted weight and girth measurement error rates achieved were low and broadly equivalent between the manual and digital measurements. Median length measurements extracted from the digital images at each measurement time point were significantly greater by between 2 and 13 mm than the equivalent manual length measurements. Previous work on digital measurements in fish morphometry has shown significant variances in the nature of the data produced by people using both manual digital and physical workflows (Petrtyl et al., 2014). With regard to manual measurements, documented sources of error include variations in the way in which the jaws and tail are manipulated during measurement (Mous et al., 1995). Given the differences between the manual and image-based measurements demonstrated in this study, we suggest the relaxed nature of both the jaws and tail fork during image capture as a probable cause of this difference. Regardless, this error is low at a maximum of approximately 2.7%, which is less than the 5.5%–7.6% reported in a multi species study by Bravata et al. (2020) and suggests that high-throughput algorithmically derived measurements will likely offer the highest quality and most repeatable representations of a population—especially for large populations.

4.4 | Individualising fish measurements highlights important structural features in fish populations

The population growth visualised in Figure 5 showed an overall biomass growth between each of the measurements taken, with a small but noticeable bimodal distribution developing in November/December 2019. Expressing individual fish growth measurements as a change from previous (Figure 6) highlighted an important feature in the population structure that developed between October and November/December 2019. The bimodal distribution in the population at the end of the study was more evident in Figure 6, and it was also clear that the lower subpopulation lost body mass and reduced in girth through this period. This loss of body mass was clear in both the manually measured weights and the digital image-based weight and girth predictions. As would be expected in the case of loss of body mass, no loss of length was measured. This demonstrates the additional

structural population knowledge gained by tracking individual fish growth measurements, which is key for successful research and breeding programmes, and the ease with which this information can be collected and analysed through the capture and linkage of digital images through to harvest. With regard to subsampling from larger populations, previous studies have noted biases and errors, particularly in large aquaculture environments (Aunsmo et al., 2013; Nilsson & Folkedal, 2019). The detection of weight loss within a subpopulation in large aquaculture environments presents a challenge as this information can be concealed by continued growth of other individuals in the population. The use of sampling strategies such as those modelled for disease detection by de Blas et al. (2020) may allow for such a detection. The use of individually identified sentinel fish in the population using tagging tools similar to those of Føre et al. (2017) may offer a means of detecting this with reduced sampling numbers however and warrants further investigation.

4.5 | Opportunities arising from digital image-based phenotypic measurements

The use of digital images to capture and store fish phenotypic measurements/records offers many advantages over traditional husbandry measurement workflows as it accurately captures and stores multiple externally visible phenotypic traits simultaneously. If used continuously as a monitoring tool during population grow-out, this approach has the potential to deliver high-quality individualised and population-level growth data. With effective archival of these images, the traits they contain remain accessible for future measurement, either through manual assessment or algorithmically, and they can be effectively linked to other data sources. Furthermore, the development of biometric identification such as that demonstrated for Atlantic salmon by Cisar et al. (2021) may allow individual fish to be tracked without invasive tags.

5 | CONCLUSIONS

Here, we have demonstrated a simple, low-cost accessible image capture system capable of operating in wet environments that allows for live, moderately anaesthetised fish to have high-quality images captured repeatedly during their growth cycle as phenotypic records, using less labour resources. We have shown that the data are comparable in quality to those generated through manual measurement workflows. Furthermore, once the data have been captured, morphometric measurements can be produced and linked to individual fish through automated software pipelines written in the Python programming language—in this case using PIT tags. Potential applications include research trials and aquaculture breeding and production programmes wishing to apply automated growth assessments of all the fish being evaluated. Finally, we provide clear evidence that the individualisation of fish growth data allows insights into fish growth and population structures that are not clearly visible in anonymised size measurements.

ACKNOWLEDGEMENTS

We would like to acknowledge all the Plant & Food Research staff who have been involved in the development of image-based solutions for finfish species over the last years, particularly Belinda Timms, and the hard work of the staff in the Cawthron Institute's Finfish Research Centre. This work was funded by the Ministry of Business, Innovation and Employment through the Endeavour fund "Feed-efficient salmon for the future" (CAWX1606) and by the New Zealand Government via the Ngā Pou Rangahau platform, a research framework developed by the New Zealand Institute for Plant and Food Research Limited and supported by a Strategic Science Investment Fund grant from the Ministry of Business, Innovation and Employment.

CONFLICTS OF INTEREST

The authors declare no conflict of interest.

ETHICS STATEMENT

All procedures involving animals were done according to the approved animal ethics protocol AEC2018 CAW01.

AUTHOR CONTRIBUTIONS

Conceptualisation, *data curation*, *formal analysis*, *methodology*, *software*, *visualisation*, *writing—original draft and writing – review and editing*: Nicholas P. L. Tuckey. *Software*: David T. Ashton, Jiakai Li and Harris T. Lin. *Investigation*, *methodology*, *resources and writing—review and editing*: Seumas P. Walker. *Conceptualisation*, *funding acquisition*, *investigation*, *methodology*, *resources and writing—review and editing*: Jane E. Symonds. *Conceptualisation*, *funding acquisition*, *writing—original draft and writing—review and editing*: Maren Wellenreuther.

FUNDING STATEMENT

This work was funded by the Ministry of Business, Innovation and Employment through the Endeavour fund "Feed-efficient salmon for the future" (CAWX1606) and by the New Zealand Government via the Nga Pou Rangahau platform, a research framework developed by the New Zealand Institute for Plant and Food Research Limited and supported by a Strategic Science Investment Fund grant from the Ministry of Business, Innovation and Employment.

DATA AVAILABILITY STATEMENT

The data that support the findings of this study are available from the corresponding author upon request.

PEER REVIEW

The peer review history for this article is available at https://publons.com/publon/10.1002/aff2.66.

ORCID

Nicholas P. L. Tuckey https://orcid.org/0000-0003-1437-636X

REFERENCES

Anaconda Software Distribution (2016) Computer software. Vers. 2-2.4.0. Anaconda Web. Available from https://anaconda.com. [Accessed 2 Nov 2021].

Andrialovanirina, N., Ponton, D., Behivoke, F., Mahafina, J. & Leopold, M. (2020) A powerful method for measuring fish size of small-scale fishery catches using ImageJ. *Fish. Res.*, 223, 105425. Available from https://doi.org/10.1016/j.fishres.2019.105425

Aquaculture New Zealand (2020) Aquaculture for New Zealand: a sector overview with key facts and statistics for 2020. Nelson, New Zealand.

Aunsmo, A., Skjerve, E. & Midtlyng, P.J. (2013) Accuracy and precision of harvest stock estimation in Atlantic salmon farming. *Aquaculture*, 396, 113–118. Available from https://doi.org/10.1016/j.aquaculture.2013.03.001

Balaban, M.O., Chombeau, M., Cırban, D. & Gümüş, B. (2010a) Prediction of the weight of Alaskan pollock using image analysis. *J. Food Sci.*, 75, E552–E556. Available from https://doi.org/10.1111/j.1750-3841.2010.01813.x

Balaban, M.O., Ünal Şengör, G.F., Soriano, M.G. & Ruiz, E.G. (2010b) Using image analysis to predict the weight of Alaskan salmon of different species. *J. Food Sci.*, 75, E157–E162. Available from https://doi.org/10.1111/j.1750-3841.2010.01522.x

Beddow, T.A., Ross, L.G. & Marchant, J.A. (1996) Predicting salmon biomass remotely using a digital stereo-imaging technique. *Aquaculture*, 146, 189–203. Available from https://doi.org/10.1016/S0044-8486(96)01384-1

Benjamini, Y. & Hochberg, Y. (1995) Controlling the false discovery rate: A practical and powerful approach to multiple testing. *J. R. Stat. Soc. Ser. B Methodol.*, 57, 289–300. Available from https://doi.org/10.1111/j.2517-6161.1995.tb02031.x

Bradski, G. (2000) The OpenCV Library. Dr Dobbs J. Softw. Tools.

Bravata, N., Kelly, D., Eickholt, J., Bryan, J., Miehls, S. & Zielinski, D. (2020) Applications of deep convolutional neural networks to predict length, circumference, and weight from mostly dewatered images of fish. *Ecol. Evol.*, 10, 9313–9325. Available from https://doi.org/10.1002/ece3.6618

Cisar, P., Bekkozhayeva, D., Movchan, O., Saberioon, M. & Schraml, R. (2021) Computer vision based individual fish identification using skin dot pattern. *Sci. Rep.*, 11, 16904. Available from https://doi.org/10.1038/s41598-021-96476-4

de Blas, I., Muniesa, A., Vallejo, A. & Ruiz-Zarzuela, I. (2020) Assessment of sample size calculations used in aquaculture by simulation techniques. *Front. Vet. Sci.*, 7, 253.

Fernandes, A.F.A., Turra, E.M., de Alvarenga, E.R., Passafaro, T.L., Lopes, F.B., Alves, G.F.O., Singh, V. & Rosa, G.J.M. (2020) Deep Learning image segmentation for extraction of fish body measurements and prediction of body weight and carcass traits in Nile tilapia. *Comput. Electron. Agric.*, 170, 105274. Available from https://doi.org/10.1016/j.compag.2020.105274

Føre, M., Frank, K., Dempster, T., Alfredsen, J.A. & Høy, E. (2017) Biomonitoring using tagged sentinel fish and acoustic telemetry in commercial salmon aquaculture: a feasibility study. *Aquac. Eng.*, 78, 163–172. Available from https://doi.org/10.1016/j.aquaeng.2017.07.004

Gjedrem, T. & Robinson, N. (2014) Advances by selective breeding for aquatic species: a review. *Agric. Sci.*, 5, 1152–1158. Available from https://doi.org/10.4236/as.2014.512125

Gjedrem, T. & Rye, M. (2018) Selection response in fish and shellfish: a review. *Rev. Aquac.*, 10, 168–179. Available from https://doi.org/10.1111/raq.12154

Houston, R. & Macqueen, D. (2019) Atlantic salmon (*Salmo salar* L.) genetics in the 21st century: taking leaps forward in aquaculture and biological understanding. *Anim. Genet.*, 50, 3–14. Available from https://doi.org/10.1111/age.12748

Hunter, J.D. (2007) Matplotlib: a 2D graphics environment. *Comput. Sci. Eng.*, 9, 90–95. Available from https://doi.org/10.1109/MCSE.2007.55

Iversen, M., Finstad, B., McKinley, R.S. & Eliassen, R.A. (2003) The efficacy of metomidate, clove oil, Aqui-S (TM) and Benzoak (R) as anaesthetics in Atlantic salmon (*Salmo salar* L.) smolts, and their potential stress-reducing capacity. *Aquaculture*, 221, 549–566.

Kause, A., Tobin, D., Houlihan, D.F., Martin, S.A.M., Mäntysaari, E.A., Ritola, O. & Ruohonen, K. (2006) Feed efficiency of rainbow trout can be improved through selection: different genetic potential on alternative diets1. *J. Anim. Sci.*, 84, 807–817. Available from https://doi.org/10.2527/2006.844807x

Luzuriaga, D., Balaban, M. & Yeralan, S. (1997) Analysis of visual quality attributes of white shrimp by machine vision. *J. Food Sci.*, 62, 113–118. Available from https://doi.org/10.1111/j.1365-2621.1997.tb04379.x

Mous, P.J., Goudswaard, P.C., Katunzi, E.F.B., Budeba, F.W., Witte, F. & Ligtvoet, W. (1995) Sampling and measuring. *Fish stocks and fisheries of Lake Victoria: a handbook for field observations*. Cardigan, UK: Samara Publishing Limited, pp. 55–82.

Murata, O., Miyashita, S., Izumi, K., Maeda, S., Kato, K. & Kumai, H. (1996) Selective breeding for growth in red sea bream. *Fish. Sci.*, 62, 845–849. Available from https://doi.org/10.2331/fishsci.62.845

Navarro, A., Lee-Montero, I., Santana, D., Henriquez, P., Ferrer, M., Morales, A., Soula, M., Badilla, R., Negrin-Baez, D., Zamorano, M. & Afonso, J. (2016) IMAFISH_ML: a fully-automated image analysis software for assessing fish morphometric traits on gilthead seabream (*Sparus aurata* L.), meagre (*Argyrosomus regius*) and red porgy (*Pagrus pagrus*). *Comput. Electron. Agric.*, 121, 66–73. Available from https://doi.org/10.1016/j.compag.2015.11.015

Navarro, A., Zamorano, M.J., Hildebrandt, S., Ginés, R., Aguilera, C. & Afonso, J.M. (2009) Estimates of heritabilities and genetic correlations for growth and carcass traits in gilthead seabream (*Sparus auratus* L.), under industrial conditions. *Aquaculture*, 289, 225–230. Available from https://doi.org/10.1016/j.aquaculture.2008.12.024

Nilsson, J. & Folkedal, O. (2019) Sampling of Atlantic salmon *Salmo salar* from tanks and sea cages is size-biased. *Aquaculture*, 502, 272–279. Available from https://doi.org/10.1016/j.aquaculture.2018.12.053

Petrtyl, M., Kalous, L. & Memis, D. (2014) Comparison of manual measurements and computer-assisted image analysis in fish morphometry. *Turk. J. Vet. Anim. Sci.*, 38, 88–94. Available from https://doi.org/10.3906/vet-1209-9

R Core Team (2021) *R: A language and environment for statistical computing*. R Foundation for Statistical Computing.

Schraml, R., Hofbauer, H., Jalilian, E., Bekkozhayeva, D., Saberioon, M., Cisar, P. & Uhl, A. (2021) Towards fish individuality-based aquaculture. *IEEE Trans. Ind. Inform.*, 17, 4356–4366. Available from https://doi.org/10.1109/TII.2020.3006933

Seabold, S. & Perktold, J. (2010) statsmodels: Econometric and statistical modeling with python. In: Proceedings of the 9th Python in Science Conference, June 28–July 3. Austin, Texas.

Sengor, G.F.U., Balaban, M.O., Topaloglu, B., Ayvaz, Z., Ceylan, Z. & Dogruyol, H. (2019) Color assessment by different techniques of gilthead seabream (*Sparus aurata*) during cold storage. *Food Sci. Technol.*, 39, 696–703. Available from https://doi.org/10.1590/fst.02018

Shortis, M.R., Ravanbakhsh, M., Shafait, F. & Mian, A. (2016) Progress in the automated identification, measurement, and counting of fish in underwater image sequences. *Mar. Technol. Soc. J.*, 50, 4–16. Available from https://doi.org/10.4031/mtsj.50.1.1

SriHari, M., Bhutia, R.N., Kathirvelpandian, A., Sharma, R., Ramteke, K.K., Sreekanth, G.B. & Abidi, Z.J. (2019) Differentiation in morphometric traits of Chanos chanos stocks along the Indian coast. *Indian J. Geo-Mar. Sci.*, 48, 233–238.

Stien, L.H., Nilsson, J., Bui, S., Fosseidengen, J.E., Kristiansen, T.S., Overli, O. & Folkedal, O. (2017) Consistent melanophore spot patterns allow long-term individual recognition of Atlantic salmon *Salmo salar*. *J. Fish Biol.*, 91, 1699–1712. Available from https://doi.org/10.1111/jfb.13491

Stoskopf, M. & Posner, L.P. (2008) Anesthesia and restraint of laboratory fish. In: Fish, R.E., Brown, M.J., Danneman, P.J. & Karas, A.Z. (Eds.). *Anesthesia and analgesia in laboratory animals* (2nd ed.). San Diego: Academic Press, pp. 519–534. Available from https://doi.org/10.1016/B978-012373898-1.50025-5

Takacs, P., Vital, Z., Ferincz, A. & Staszny, A. (2016) Repeatability, reproducibility, separative power and subjectivity of different fish morphometric analysis methods. *Plos One*, 11, e0157890. Available from https://doi.org/10.1371/journal.pone.0157890

Teletchea, F. & Fontaine, P. (2014) Levels of domestication in fish: implications for the sustainable future of aquaculture. *Fish Fish.*, 15, 181–195. Available from https://doi.org/10.1111/faf.12006

The pandas development team (2020) pandas-dev/pandas: pandas. Zenodo.

Viazzi, S., Van Hoestenberghe, S., Goddeeris, B.M. & Berckmans, D. (2015) Automatic mass estimation of Jade perch Scortum barcoo by computer vision. *Aquac. Eng.*, 64, 42–48. Available from https://doi.org/10.1016/j.aquaeng.2014.11.003

Waskom, M. & the Seaborn Development Team. (2020) mwaskom/seaborn. Zenodo. Available from https://doi.org/10.5281/zenodo.592845. [Accessed 2 Nov 2021].

Zion, B. (2012) The use of computer vision technologies in aquaculture—a review. *Comput. Electron. Agric.*, 88, 125–132. Available from https://doi.org/10.1016/j.compag.2012.07.010

How to cite this article: Tuckey, N.P.L., Ashton, D.T., Li, J., Lin, H.T., Walker, S.P., Symonds, J.E. & Wellenreuther, M. (2022) Automated image analysis as a tool to measure individualised growth and population structure in Chinook salmon (*Oncorhynchus tshawytscha*). *Aquaculture, Fish and Fisheries*, 1–12. https://doi.org/10.1002/aff2.66